Acta Cryst. (1997). A53, 615–631

De Nive Sexangula Stellata

ALOYSIO JANNER

Institute for Theoretical Physics, University of Nijmegen, Toernooiveld, 6525 ED Nijmegen, The Netherlands. E-mail: alo@sci.kun.nl

(Received 12 February 1997; accepted 23 April 1997)

Dedicated to Professor T. Janssen on the occasion of his 60th birthday

Abstract

Scaling symmetry is observed in snow crystals as a relation between hexagons inscribing and circumscribing hexagonal star polygons. These patterns are revealed by a characteristic distribution of clear spots (pores) and of dark lines. The new symmetry demonstrates the possible relevance of non-Euclidean (multimetrical) crystallography for crystals in nature. The multimetrical space group of the (ideal) ice structure is derived and the morphology of snow crystals is interpreted on the basis of the corresponding crystallographic point group of infinite order. The morphological importance of a set of basic structural sites, indexed according to points of a macroscopic hexagonal lattice, is discussed. Rules are formulated for the growth forms of snow crystals of the dendritic and of the facet type.

1. Introduction

The sixfold symmetry one admires in snow crystals moved Kepler to find an explanation of the *six-cornered snowflake* in terms of an underlying microscopic structure. It was the year 1611. Kepler could associate a hexagonal symmetry to a close packing of equal spheres but as he could not account for the mainly planar structure of snowflakes he did not published his work as a scientific paper but as a Christmas gift *Strena Seu De Nive Sexangula* dedicated *ad illustrem sacrae caesareae maiestatis consiliarium imperialem aulicum, dominum Ioannem Matthaeum Wackherium* at the court of the Emperor Rudolf in Prague (Kepler, 1611). Despite his impression of having failed, his contribution was relevant and far ahead of his time. His work inspired generations of investigators. Nowadays, one is aware of the complexity of physical phenomena associated with such a simple molecule as H_2O, in water, in ice and in snow (Ben-Jacob, 1993; Bernal & Fowler, 1933).

The title adopted from Kepler reflects the central idea of the present contribution, which bases the symmetry of snow crystals on the *hexagonal star polygon* (the hexagram) instead of on the hexagon only. This is the surprising result of an attempt to convince the participants of the ACA meeting held in Atlanta in 1994 that there is only *one crystallography*, despite the present paradoxical situation, where aperiodic crystals are described in terms of higher-dimensional lattice-periodic structures, where quasicrystals (which are discrete) involve crystallographic scaling symmetries and where non-Euclidean crystallography can be applied to normal crystals (which are Euclidean objects) (Janner, 1995*a*).

It is easily understandable that a more comprehensive crystallography, which takes all that into account, can be considered as an interesting mathematical construction (or at most a geometrical one) far from any physical reality. Amazingly enough (as we hope to be able to show), snow, 'the beautiful snow' as Bentley & Humphreys (1931) write in their marvelous photographic collection, reveals these new crystallographic aspects at a macroscopic scale in a way compatible with the microscopic structure of ice. In other words, the morphology of snow crystals (in a two-dimensional approximation) brings some evidence that non-Euclidean crystallographic symmetries combined with the Euclidean ones play a role in nature.

What will be presented here is the logical consequence of previous developments. Conceptually, hexagrammal symmetry has the same foundation as the pentagrammal symmetry observed in the Fourier map of the decagonal phase of $Al_{78}Mn_{22}$ (Janner, 1992; Steurer, 1991) and in a high-resolution electron microscope (HREM) picture of the icosahedral AlMn quasicrystal phase, sent as New Year's greetings for 1986 by the colleagues of the Center for High-Resolution Microscopy of the University of Antwerpen (RUCA) (Janner, 1995*a*). At the crystallographic level of a higher-dimensional description, the scale-rotational symmetry of a self-similar pentagram is a point group generated by a fivefold circular rotation and a τ-related hyperbolic rotation [where $\tau = (1 + 5^{1/2})/2$]. The circular rotation leaves the Euclidean metric invariant, whereas the hyperbolic rotation leaves invariant an indefinite metric. This justifies the name *multimetrical* point group. The planar multimetrical symmetry of a snow crystal appears to be generated in an analogous way by a sixfold circular rotation and by a $3^{1/2}$-related hyperbolic rotation, both leaving the hexagonal lattice invariant. This group is the point group of a three-dimensional multimetrical space group leaving the (ideal) structure of ice invariant, as discussed later.

2. Beyond the hexagonal point-group symmetry

Behind the rich morphology of snow crystals, there are intriguing structural relations not explained by the hexagonal point group $K_0 = 6/mmm$ of ice. The aim of this paper is to identify characteristics of these relations in patterns visible in snow crystals of different shapes. In this section, the approach is purely phenomenological, even if the starting motivation for searching well defined patterns had been an abstract theoretical one, as explained in the *Introduction*.

Let us consider representatives of the two main morphological snowflake types: with facets and with dendrites, respectively. The third type with hexagonal prismatic columns is not considered here because of the planar approximation adopted. This is a very rough subdivision, a finer classification has been given by Nakaya (1954). A picture of the first two samples has been published in the *Scientific American* of 1961 in an article by Mason (1961). The first crystal has a star-like dendritic form, the second one, like a flower, is of the facet type and has branches in sector form. In the first case (sample SA 1, where SA denotes the source *Scientific American*, whose permission to reproduce is gratefully acknowledged), the structural relation between two scaled hexagons appears when considering a hexagonal star polygon with vertices at the branching points of the dendrites (Fig. 1). In the second case (SA 2), two morphological elements are considered separately: black lines (Fig. 2) and light spots (Fig. 3). Again and again, one observes hexagons in vertex–vertex or vertex–mid-edge relation with hexagonal star polygons. These pictures, which suggest a scaling symmetry in

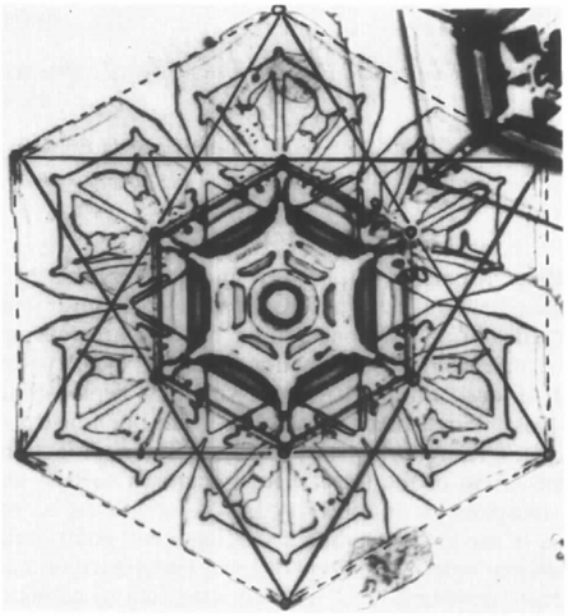

Fig. 2. Facet flower-like snow crystal (SA 2). The dark-line pattern of the external growth form shows a hexagrammal relation similar to that of Fig. 1 with an internal black hexagon. Another hexagonal star polygon of about the same size, but turned by 30° with respect to the black hexagon is also visible, somewhat in the background. (Courtesy of *Scientific American*.)

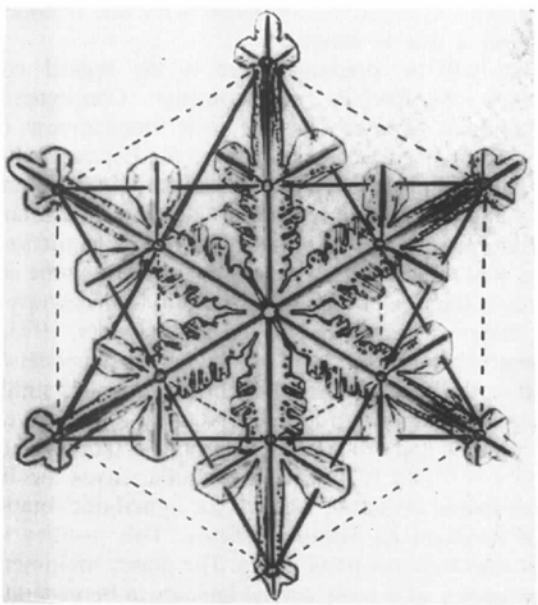

Fig. 1. Dendritic star-like snow crystal (SA 1) with branching points belonging to a hexagonal star polygon and arranged according to two scaled hexagons with the same orientation. The larger one circumscribes the hexagram, the smaller one is inscribed in it. In the real crystal, small deviations are observed from the ideal structural relations indicated here. (Courtesy of *Scientific American*.)

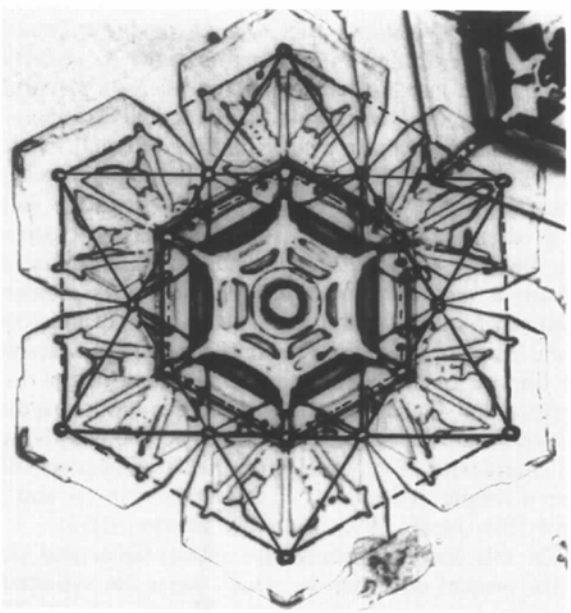

Fig. 3. Same crystal as in Fig. 2. The structural relations shown are among light spot-like regions. In addition to the hexagrammal vertex–mid-edge relation of two scaled hexagons, there is an additional hexagon in vertex–vertex relation. (Courtesy of *Scientific American*.)

addition to the hexagonal one, were presented at the Atlanta meeting (Gonev & Kraus, 1994).

To show that what has been described is not accidental, a third sample is presented, taken from the well known book by Bentley & Humphreys (1931) and denoted as BH 95.11. (The notation BH 95.11 indicates the 11th snow crystal from the top on page 95 of the book. This picture is reproduced, and the other ones which follow, by courtesy of Dover.) It is a snow crystal with light spots easily identified. A set of them forms a sequence of three scaled hexagonal star polygons in vertex–vertex relation with the corresponding hexagons (Fig. 4). A fourth snowflake is presented here because it shows dark lines drawing a hexagonal star polygon in a vertex–mid-edge relation with a hexagon (Fig. 5). All these snow crystals, together with a few more samples taken from Bentley & Humphreys, will be analyzed later.

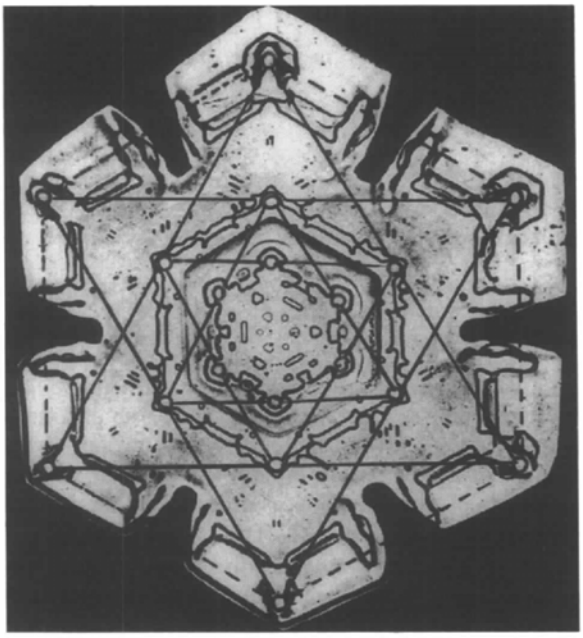

Fig. 4. Snow crystal of the facet type (BH 95.11) with a set of light spots arranged according to three scaled hexagons in hexagrammal scaling relation. (Courtesy of Dover.)

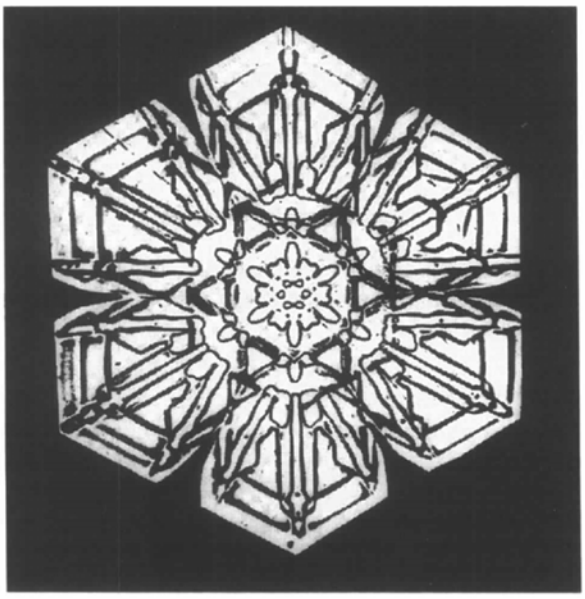

Fig. 5. Snow crystal (BH 141.11) with a central pattern of dark lines forming a hexagonal star polygon. (Courtesy of Dover.)

3. A multimetrical crystallographic approach

The pentagrammal scale-rotational symmetry observed in decagonal quasicrystals can be expressed by crystallographic point-group transformations represented by four-dimensional integral invertible matrices. This is not the case for the scale-rotational hexagrammal symmetries, even if one can derive them from a set of scaled hexagonal lattices, because the corresponding symmetry transformations are not unimodular. It is, however, not the end of the story. As already recognized in another context, a hexagonal lattice also has non-Euclidean crystallographic point-group symmetries, which are discrete hyperbolic rotations (Janner, 1991*b*). Furthermore, crystals occurring in nature can be invariant (in the point-atom approximation) with respect to multimetrical space groups (Janner, 1991*a*; Janner, 1995*b*). Let us, therefore, consider whether one can assign such a symmetry group to the structure of ice and then try to associate the corresponding multimetrical point group to the macroscopic growth forms of snow crystals.

3.1. *The multimetrical symmetry of ice*

The space group of ice is $P6_3/mmc$. One finds the O atoms on the $4(f)$ Wyckoff positions. According to the Pauling model (Pauling, 1935) and a neutron diffraction study of heavy ice (Peterson & Levy, 1957), half of the H atoms (H_1) are also on $4(f)$ and half (H_2) on the $12(k)$ positions.

A multimetrical extension of the Euclidean space group requires, in general, an idealization of the structure because the enlarged symmetry only applies to a point-atom approximation and this implies for the real crystal the possibility of a symmetry-breaking deformation. The ideal structure should, therefore, be related to a substantial increase of symmetry with respect to that of the real crystal. In the present case, the simplest extension of the Euclidean symmetry is represented by a hyperbolic rotation L_z around the hexagonal axis, leaving the lattice invariant. With respect to the lattice basis $a = \{a_1, a_2, a_3\}$:

$$a_1 = a(1, 0, 0), \quad a_2 = a(-1/2, 3^{1/2}/2, 0),$$

$$a_3 = c(0, 0, 1), \qquad (1)$$

Table 1. *Parameters and symmetry groups of ideal ice structures*

Positions	Parameters	$P6_3/mmc$	$P6_3/mmcL_{z\frac{1}{2}}$	$P6_3/mmcL_{z\frac{1}{2}}L_yL_{x\frac{1}{2}}$
	a/c	1.6297	1.6297	$1.633 = (8/3)^{1/2}$
O at $4(f)$	z_0	0.0625	$0.0625 = 1/16$	$0.0625 = 1/16$
H_1 at $4(f)$	z_1	0.198	0.198	$0.1875 = 3/16$
H_2 at $12(k)$	z_2	0.0172	0.0172	0.0 or 0.0625
	x_2	0.4545	0.5	0.5

L_z has the matrix form

$$L_z(a) = \begin{pmatrix} 3 & 1 & 0 \\ 2 & 1 & 0 \\ 0 & 0 & 1 \end{pmatrix}. \tag{2}$$

The transformation $L_{z\frac{1}{2}} = \{L_z \mid 0, 0, \frac{1}{2}\}$ leaves the Wyckoff positions $4(f)$ of $P6_3/mmc$ invariant. Invariance of the $12(k)$ positions $x, 2x, z, \ldots, x, \bar{x}, \bar{z} + \frac{1}{2}$ is ensured by the condition $6x = 0 \bmod 1$. The best approximation to the experimental value of $x = 0.4545$ is $x = \frac{1}{2}$. As for ice, the a/c ratio is very near to that of a hexagonal close-packing lattice Λ_{hcp}, we also consider the hyperbolic rotations L_x and L_y around the x and y axes, respectively, which leave Λ_{hcp} invariant:

$$L_x(a) = \begin{pmatrix} 1 & 8 & 16 \\ 0 & 17 & 32 \\ 0 & 9 & 17 \end{pmatrix}, \quad L_y(a) = \begin{pmatrix} 49 & -24 & 80 \\ 0 & 1 & 0 \\ 30 & -15 & 49 \end{pmatrix}. \tag{3}$$

One then finds that the $4(f)$ Wyckoff positions $\frac{1}{3}, \frac{2}{3}, z$; $\frac{2}{3}, \frac{1}{3}, z + \frac{1}{2}$; $\frac{2}{3}, \frac{1}{3}, \bar{z}$; $\frac{1}{3}, \frac{2}{3}, \bar{z} + \frac{1}{2}$ are left invariant by $L_{x\frac{1}{2}} = \{L_x \mid 0, 0, \frac{1}{2}\}$ and by $L_y = \{L_y \mid 0, 0, 0\}$ for the discrete values of $16z = 0 \bmod 1$. To see this, consider for example the action of $L_{x\frac{1}{2}}$ on the atomic position $\frac{1}{3}, \frac{2}{3}, z$, modulo the lattice translations:

$$\{L_x|0, 0, \tfrac{1}{2}\}(\tfrac{1}{3}, \tfrac{2}{3}, z) \simeq (\tfrac{2}{3} + 16z, \tfrac{1}{3} + 32z, \tfrac{1}{2} + 17z). \tag{4}$$

Invariance requires $16z = 0 \bmod 1$, leading to the position $(\frac{2}{3}, \frac{1}{3}, z + \frac{1}{2})$. The O-atom positions satisfy this condition as $z_0 = 0.0625 = 1/16$ and the first half of the H atoms H_1 also, if one adopts the value $z_1 = 3/16 = 0.1875$ instead of the observed one of 0.198. Invariance for the positions $12(k)$ of the second half of the H atoms H_2, assuming $x = \frac{1}{2}$ as above because of L_z, also implies $16z = 0 \bmod 1$. A fairly good approximation of the observed value $z_2 = 0.0172$ is $z = 0$. In this case, the four H atoms are distributed among the $6(g)$ positions. For keeping the $12(k)$ positions, one needs the less good approximation of $z = 1/16 = 0.0625$. Adopting these values for an ideal ice structure gives as symmetry the multimetrical space group

$$G_1 = \left\langle \Lambda_{\text{hcp}}, R_{z\frac{1}{2}}, m_x, m_y, m_{z\frac{1}{2}}, L_{z\frac{1}{2}}, L_y, L_{x\frac{1}{2}} \right\rangle = P6_3/mmc\, L_{z\frac{1}{2}} L_y L_{x\frac{1}{2}}, \tag{5}$$

whereas if for the idealized structure one only changes the parameter x_2 of the H_2 positions to the value $x_2 = 0.5$, the symmetry is smaller and given by

$$G_2 = \langle \Lambda_{\text{hex}}, R_{z\frac{1}{2}}, m_x, m_y, m_{z\frac{1}{2}}, L_{z\frac{1}{2}} \rangle = P6_3/mmc\, L_{z\frac{1}{2}}. \tag{6}$$

If no idealization at all is made, the symmetry remains the Euclidean one $P6_3/mmc$. In Table 1, the parameters are indicated leading to these symmetry groups (which are in a group–subgroup relation). Note that all three space groups are invariance groups for the O-atom positions.

The first case $P6_3/mmc$ is disregarded because we are looking for more than plain hexagonal symmetry. The other two groups imply the same consequences for the planar symmetry of snow crystals. It is, therefore, sufficient to adopt the value $x_2 = 0.5$ for the H_2 positions. This leads to $P6_3/mmc\, L_{z\frac{1}{2}}$, whose point group is

$$K_2 = \langle R_z, L_z, m_x, m_y, m_z \rangle = 6(4)mmm, \tag{7}$$

where (4) stands for the generator L_z (which, as hyperbolic rotation in the plane, has trace 4 and this value fixes by $2\cosh\chi = 4$ the rotation angle χ). The corresponding two-dimensional point group is denoted by

$$K = \langle R, L, m_y \rangle = 6(4)m. \tag{8}$$

The challenge is now to recognize the effects of this non-Euclidean point group in the (Euclidean) morphology of planar snow crystals.

3.2. *The point group 6(4)m*

The two-dimensional point group $K = 6(4)m$ is generated by three reflections:

$$m_1(a) = \begin{pmatrix} 1 & \bar{1} \\ 0 & \bar{1} \end{pmatrix}, \quad m_2(a) = \begin{pmatrix} 1 & 0 \\ 1 & \bar{1} \end{pmatrix}, \quad m_3(a) = \begin{pmatrix} \bar{1} & 0 \\ \bar{2} & 1 \end{pmatrix}, \tag{9}$$

where with respect to the previous notation $m_1 = m_y$ and the basis set a is here restricted to the two-dimensional hexagonal one. The pair m_1, m_2 generates the Euclidean subgroup $K_0 = 6m$, as $m_2 m_1 = R$. The pair m_1, m_3 generates the hyperbolic subgroup $K_h = (4)m$ as $m_1 m_3 = L$. The elements $m_2 m_3 = P_1$ and $m_3 m_1 m_2 m_1 = P_2$ generate the parabolic subgroups K_{p1} and K_{p2}, respectively:

$$K_0 = \langle R, m_1 \rangle = 6m, \quad K_h = \langle L, m_1 \rangle = (4)m,$$
$$K_{p1} = \langle RL \rangle, \quad K_{p2} = \langle L^{-1}R \rangle. \tag{10}$$

As shown in Appendix A, the group of matrices $K(a)$, obtained by expressing the point group $K = 6(4)m$ with respect to the two-dimensional hexagonal lattice basis a, is a subgroup of index four in the group $Gl(2, \mathbb{Z})$ of integral invertible two-dimensional matrices. A right coset decomposition of $Gl(2, \mathbb{Z})$ with respect to K is given by

$$Gl(2, \mathbb{Z}) = K\left[\begin{pmatrix} 1 & 0 \\ 0 & 1 \end{pmatrix} + \begin{pmatrix} 1 & 1 \\ 0 & 1 \end{pmatrix} + \begin{pmatrix} 1 & \bar{1} \\ 0 & 1 \end{pmatrix} + \begin{pmatrix} \bar{1} & 1 \\ \bar{1} & 0 \end{pmatrix}\right]. \tag{11}$$

Important for analyzing the morphology of snow crystals are sets of point-group-equivalent points, forming the orbits of $6(4)m$. The orbit of the origin consists of a single point. All other orbits are infinite sets. In order to get a better feeling of the structures involved, one can consider typical orbits of points of the hexagonal invariant lattice for few cyclic subgroups: elliptic (circular), hyperbolic and parabolic ones (Fig. 6). Once the origin is chosen, the application of $6(4)m$ to a point with rational coordinates generates a discrete set of points of a two-dimensional lattice. The rationality is implied by the process of crystallization, which ensures that this lattice, attached to the crystal growth form and denoted here Λ_{cf}, has the same orientation as the underlying microscopic lattice Λ of symmetry translations, so that

$$\Lambda_{cf} = \lambda \Lambda \tag{12}$$

for a suitable real factor λ that relates microscopic to macroscopic features and can be taken as integral. We assume accordingly that $X(1,0) = Na_1 \simeq \lambda a_1$. All this excludes, in particular, orbits of points along the asymptotes of the hyperbolic rotations appearing in the point group. Furthermore, orbits only differing by a scaling factor and/or by a rotation are considered equivalent. Therefore, we can restrict the choice to

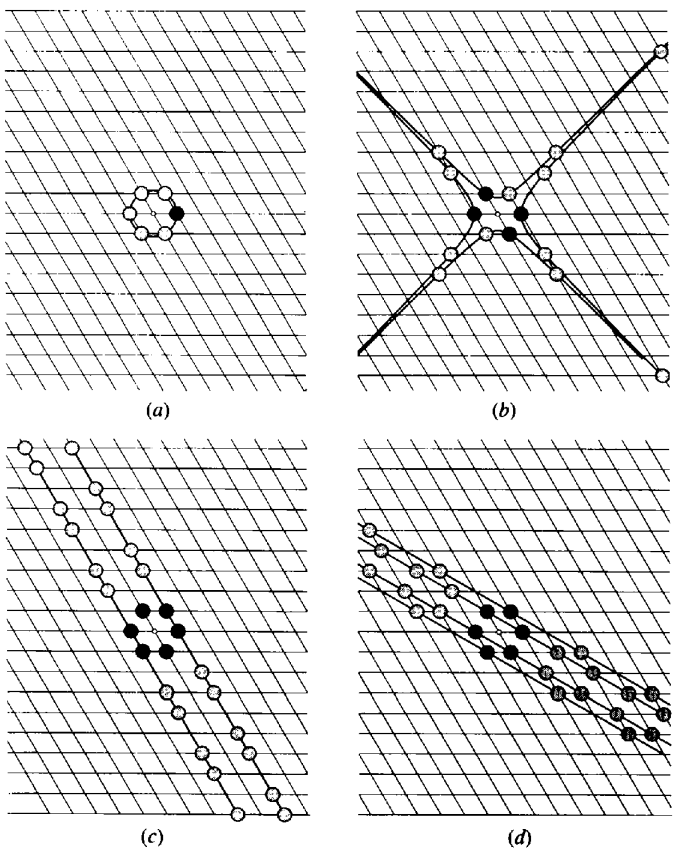

Fig. 6. Some typical orbits for cyclic subgroups of the point group $6(4)m$ leaving the hexagonal lattice invariant. (*a*) Elliptic subgroup $\langle R \rangle$. (*b*) Hyperbolic subgroup $\langle L \rangle$. (*c*) and (*d*) Parabolic subgroups $\langle P_1 \rangle$ and $\langle P_2 \rangle$, respectively.

points $X(a) = (n_1, n_2) = n_1 a_1 + n_2 a_2$ with relatively prime integral coordinates. These points form a single orbit under the group $Gl(2, \mathbb{Z})$, which decomposes into two orbits of the subgroup $6(4)m$, obtained from the points $(1, 0)$ and $(\bar{1}, 1)$, respectively (Fig. 7). This follows from the coset decomposition given above. As derived in Appendix A, the points of these two orbits can be obtained from the following selection rules among the lattice points of Λ_{cf}:

$$O_{6(4)m}(1,0) \ni (m,n) \Leftrightarrow \text{g.c.d.}(m,n) = 1 \quad \text{and} \quad (2m - n) = 1 \bmod 3 \quad \text{or} \quad (2m - n) = 2 \bmod 3 \tag{13}$$

$$O_{6(4)m}(\bar{1},1) \ni (m,n) \Leftrightarrow \text{g.c.d.}(m,n) = 1 \quad \text{and} \quad (2m - n) = 0 \bmod 3. \tag{14}$$

Of course, these two orbits are equivalent by a scale-rotation transformation. The conclusion is that it is sufficient to look at the orbit $O_{6(4)m}(1, 0)$ of $X(1, 0)$ by $6(4)m$, in addition to the trivial orbit of the origin.

It is interesting to look at the orbits of the parabolic subgroups, possibly responsible for the one-, three- and four-branched crystal forms mentioned by Nakaya (1954) (see also Frank, 1982), whereas the sixfold conjugated parabolic subgroups would give rise to the characteristic six-pointed stars, both as a growth form and as line patterns radiating from the center. In the case of K_{p1}, the star branches (and the corresponding lines) are through the vertices of a central hexagon, whereas those oriented perpendicularly to the hexagonal edges are due to being conjugated to the other parabolic subgroup K_{p2} (Fig. 8a). If complementary regions are considered, one gets a larger hexagon and the situation

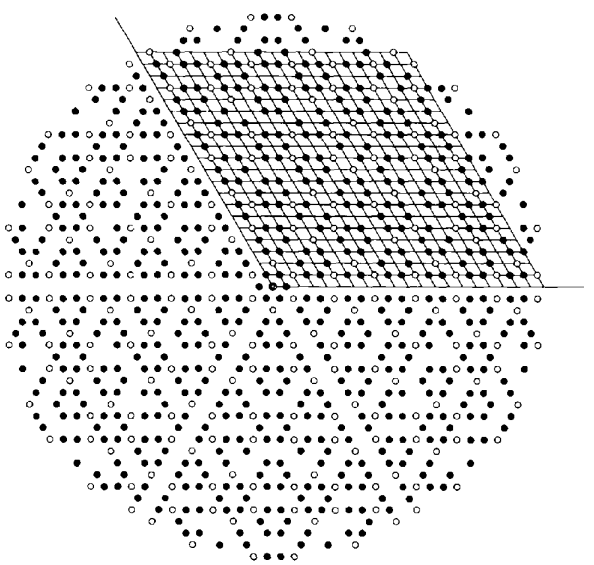

Fig. 7. Hexagonal lattice and the orbit $O_{Gl(2,Z)}(1, 0)$. The elements of this orbit are lattice points (m, n) satisfying the condition g.c.d.$(m, n) = 1$. This orbit splits into the two orbits $O_{6(4)m}(1, 0)$ and $O_{6(4)m}(\bar{1}, 1)$ for the subgroup $6(4)m$ with points indicated by filled and empty circles, respectively. Only points lying in a circle of radius 24 are shown.

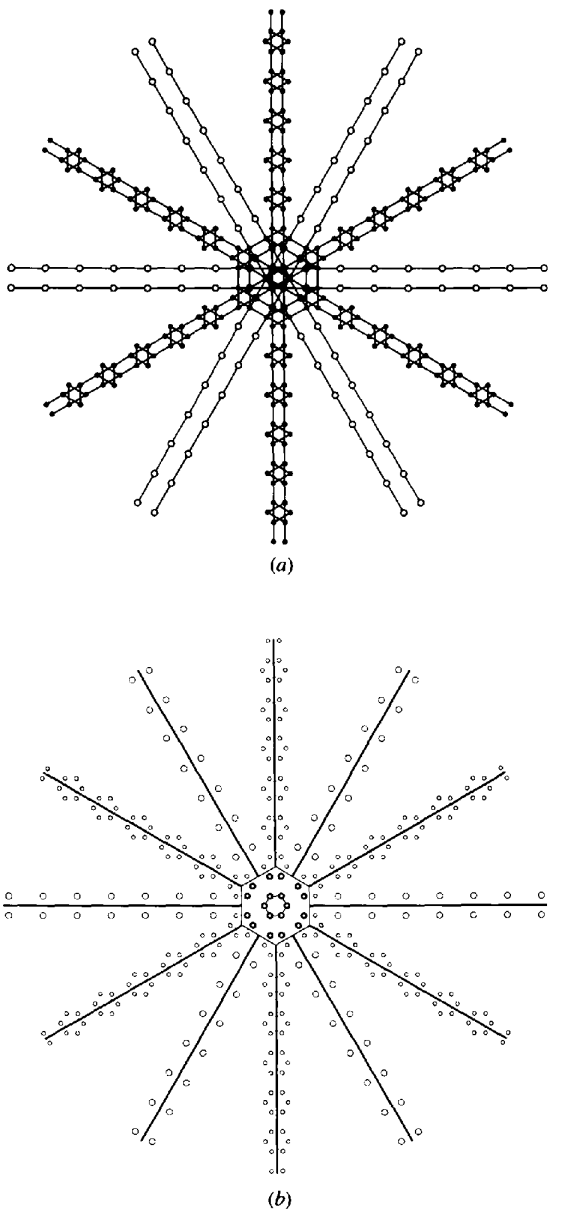

Fig. 8. (a) Orbits generated from the vertices of a central hexagon by two sets of parabolic subgroups. Those conjugated by R^k to $K_{p_2} = \langle m_3 m_1 m_2 m_1 \rangle$ for $k = 1, \ldots, 6$ give rise to the points (filled circles) of the radial patterns in the direction of the vertices of the hexagon. The others, also sixfold conjugated but to $K_{p_1} = \langle m_2 m_3 \rangle$, produce the points (empty circles) of the patterns perpendicular to the edges of the same hexagon. (b) The previous situation is reversed if one considers the complementary internal regions. Only the points lying in the same region as in Fig. 7 are shown.

is reversed (Fig. 8*b*). Examples of both cases are the sample BH 150.4 (Fig. 9*a*) and BH 151.11 (Fig. 9*b*), respectively. The orbits of both classes of conjugated parabolic subgroups together would explain the rarer case of the 12-branched type [see the cover picture of the *Handbook of Crystal Growth* (Hurle, 1993)]. If this is the case, one can understand why dodecagonal snow crystals are possible but exceptional. Apparently, these various subgroup orbits occur more frequently by the formation of internal patterns (black and white corresponding to complementary situations) observed in many snow crystal samples (Fig. 9*c*). The existence of morphologically relevant complementary regions suggests, in addition to the points of the orbit $O_{6(4)m}(1,0)$ (Fig. 10*a*), consideration of the Voronoi cells (Fig. 10*b*) and the holes (Fig. 10*c*), which are the vertices of the Voronoi cells (Conway & Sloane, 1988) of the set of orbit points. These holes, forming the set $HO_{6(4)m}(1,0)$, can be indexed by rational numbers (p,q) representing the position of the hole with respect to the crystal-form lattice Λ_{cf}. The local surrounding of a hole by orbit points is also relevant and is here expressed in terms

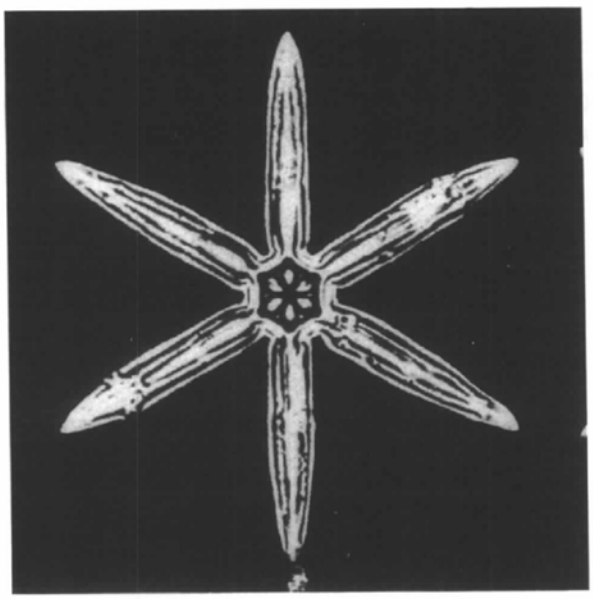

(*a*)

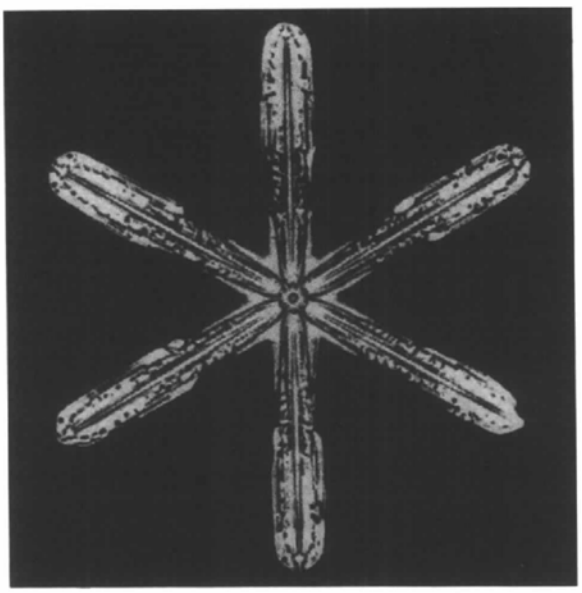

(*b*)

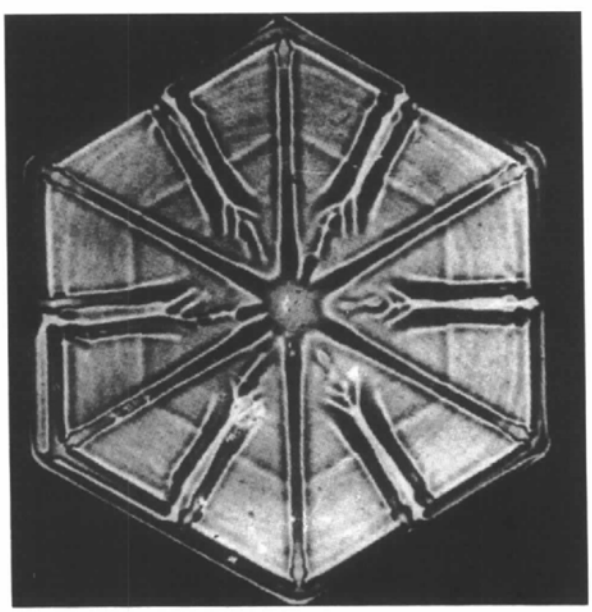

(*c*)

Fig. 9. (*a*) Six-star crystal (BH 150.4) with branches starting from the vertices of a central hexagon. (*b*) Another six-star crystal (BH 151.11) with branches starting at the mid-edge positions of the hexagon. (*c*) Snow crystal of the facet type (BH 31.11) with both sets of branches revealed by a pattern of dark (and light) internal lines. (Courtesy of Dover.)

of its *multiplicity*, given by the number of Voronoi cells at the vertex in question.

4. Growth forms and internal patterns of snowflakes

A characterization of the symmetry of snow crystals involves two different aspects. The first aspect is represented by growth forms, mainly reflected in the external shape of the crystal (which can be the result of more than one growth form). The second aspect is what we may call the internal macroscopic structure of patterns of lines and dots (pores), of light and dark regions (particularly evident in light transmission). The origin of these patterns has been considered both by Bentley & Humphreys and by Nakaya. Bentley & Humphreys say, in particular: '... By far the greater number, however, of these lines and dots on the snow crystal are due to cavities, usually empty, but sometimes partially filled with water'. According to Nakaya, these patterns arise by total reflection: ' To speak specifically about the patterns, the narrow ditches and ridges on the surface appear in black by total reflection'.

In our perspective, the patterns of both the growth forms reflect the same multimetrical point-group symmetry of a not further specified potential. In particular, the symmetry-related potential maxima (avoided by the crystallizing water molecule and by impurities) appear as light regions, whereas the darker regions arise from the complementary potential minima. One has to be aware that, when applying non-Euclidean transformations to a potential (which is a function in the Euclidean space), symmetry-related points do not have, in general, the same energy. This phenomenon is well known in the case of Bragg spots in the diffraction of a self-similar quasicrystal structure. The positions of the Bragg peaks are invariant with respect to elements

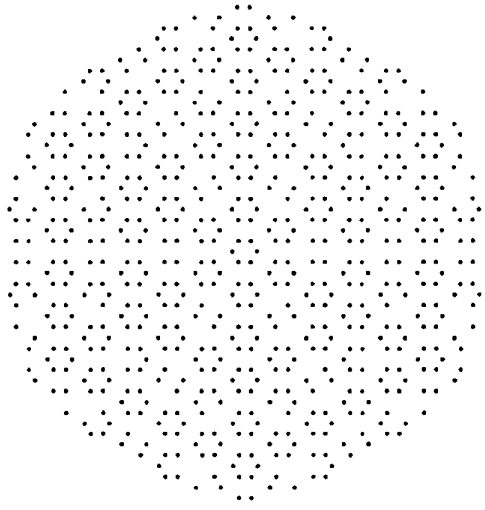

(*a*)

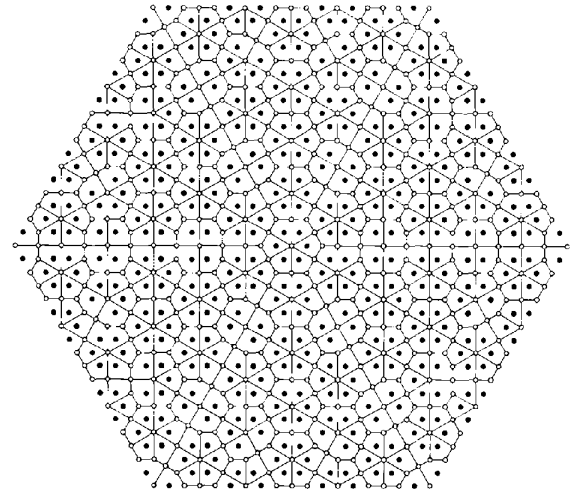

(*b*)

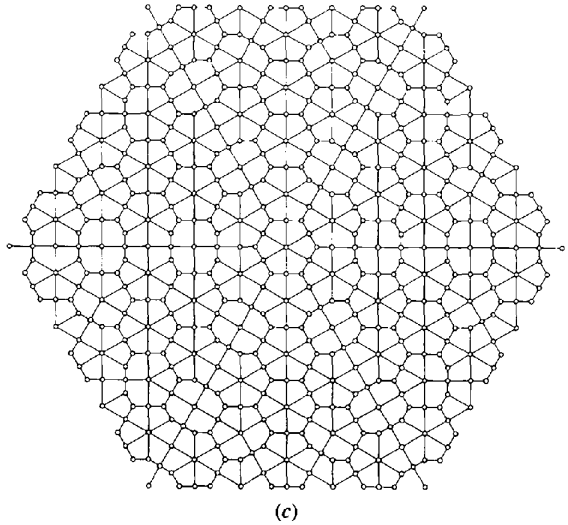

(*c*)

Fig. 10. (*a*) Points of the orbit $O_{6(4)m}(1,0)$ within a circle or radius 24. (*b*) Partition of this region in Voronoi cells. (*c*) Corresponding orbit holes, which are the vertices of the Voronoi cells.

of a scale-rotational point group. Scaling-related peaks need not have the same intensity but Bragg spots are mapped into Bragg spots, thus maxima into maxima. The idea that symmetry-related points share the same extremal character is a working hypothesis to be tested in subsequent work. Our present aim is a limited one: to show a geometrical compatibility between orbits, growth forms and internal patterns, dark and light, respectively, in the spirit of the empirical observations reported in §2.

4.1. *Snowflakes of the dendritic type*

Let us first try to interpret the structural relations of the sample SA 1 presented in Fig. 1. The growth is mainly radial but no two orbit points can occur along a given radial direction. Therefore, in this case, the orbit points have to be associated with potential maxima and the boundaries of the growth form, whereas holes represent minima of the potential along which the growth is faster, which is a general feature for this type of snowflake. The specific form of the sample considered (Fig. 11*a*) can be characterized by a star-like *skeleton* with branching at the dendritic branching points. Fig. 11(*b*) shows this skeleton in terms of a number of orbit holes, which represent *basic structural sites*. The indices of the basic structural sites for this snowflake are:

$$(0,0)\quad (4,8)\quad (8,16)\quad (10,20)\quad (8,10)\quad (12,18)\quad (15)$$

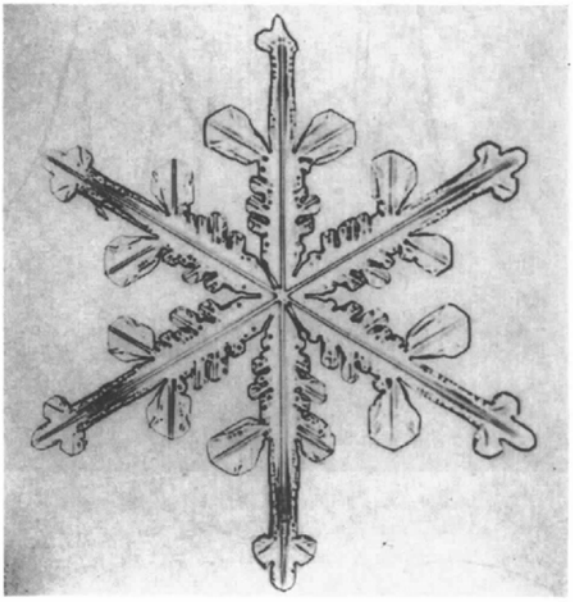

(*a*)

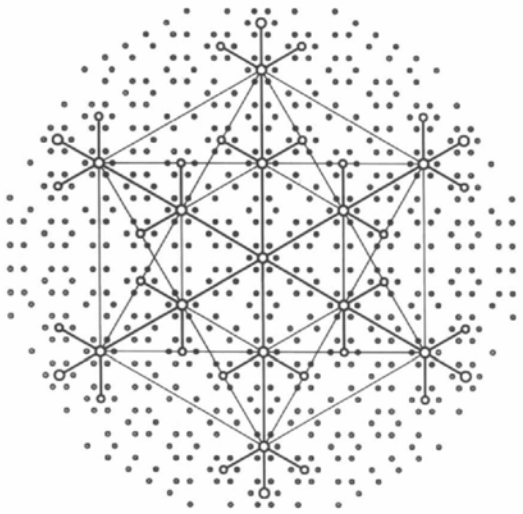

(*b*)

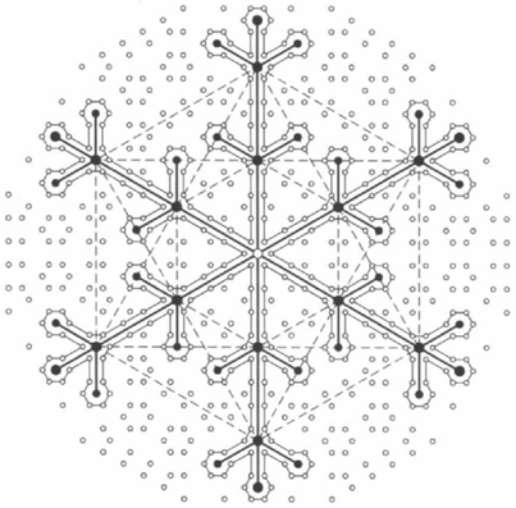

(*c*)

Fig. 11. Interpretation of the morphology of the dendritic crystal SA 1. (*a*) The crystal. (Courtesy of *Scientific American*.) (*b*) Its idealized skeleton in terms of basic structural sites (empty circles) at holes of maximal multiplicity of the orbit points (grey filled circles). One finds the same hexagrammal structural relations as indicated in Fig. 1. (*c*) The boundary of the dendrites are obtained by connecting orbit points, here indicated by empty circles.

together with their transformed ones by the hexagonal point group $6m$. With this assignment, the empirical structural relations indicated in Fig. 1 are interpreted in terms of high-multiplicity holes of $HO_{6(4)m}(1,0)$ (Fig. 11*b*). The orbit points around the skeleton then define, as expected but in a somewhat schematic way, the boundaries of the dendrites (Fig. 11*c*). In this case, the morphological form is characterized by the rational indices of points of a direct lattice and not by the rational indices of lattice planes attached to points of the reciprocal lattice, as is usually the case for non-dendritic crystals.

In order to verify that the description given does not represent a single case, two other dendritic snowflakes taken from Bentley & Humphreys are analyzed in the same way (BH 188.12 and BH 183.8). Considered are orbit points, orbit holes and basic structural sites having rational indices and defining a crystal form skeleton

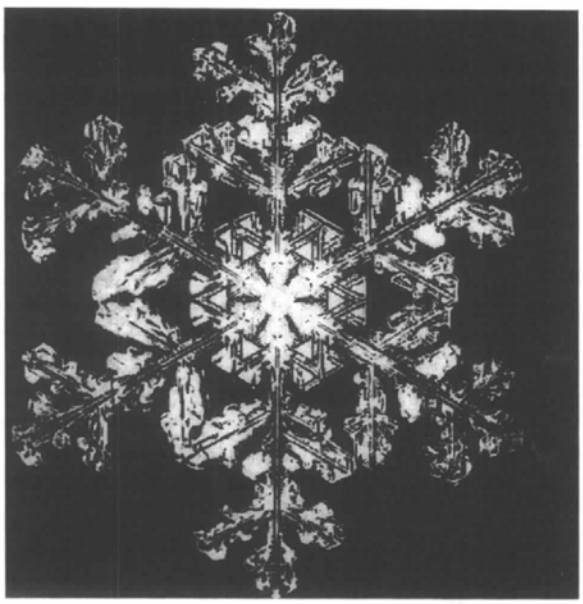

(*a*)

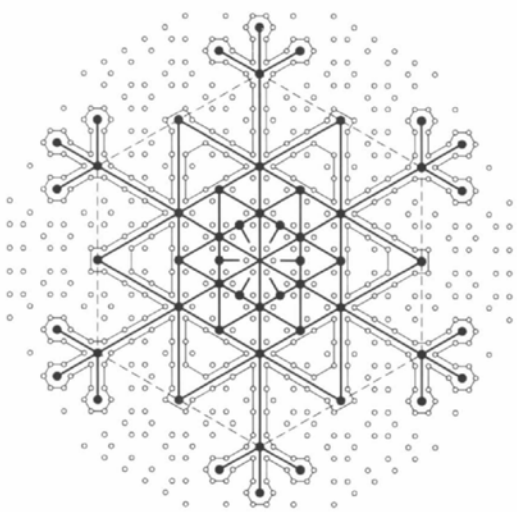

(*b*)

Fig. 12. Morphological relations in the dendritic sample BH 188.12. (*a*) The crystal. (Courtesy of Dover.) (*b*) The basic structural sites (black filled circles) at holes of the orbit points (empty circles) forming the skeleton. The crystal boundaries are drawn by connecting orbit points. The hexagrammal scaling relations are evident. Some small dendritic branches have not been included for clarity but they would also fit the same description.

(*a*)

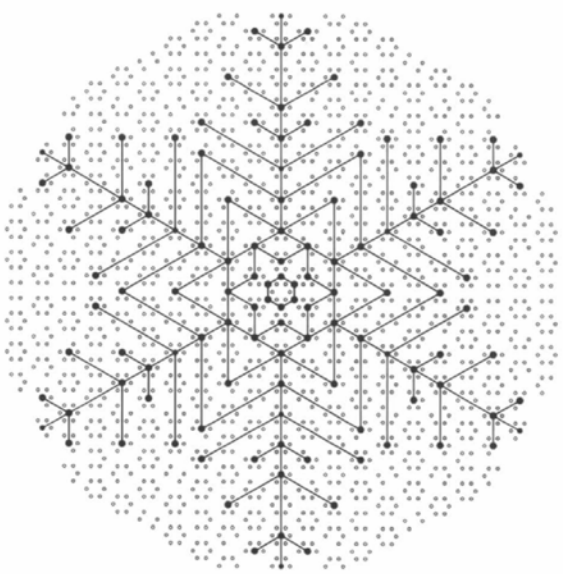

(*b*)

Fig. 13. (*a*) The snow crystal BH 183.8. (Courtesy of Dover.) (*b*) The dendritic skeleton given in terms of basic structural sites (black filled circles) at hole positions.

(Figs. 12 and 13). One finds again and again scaled hexagons in hexagrammal relation. In the first case (SA 1), there are two hexagons in vertex–vertex arrangement. In the last two samples, one distinguishes at least three hexagons in vertex–mid-edge relation with the corresponding hexagonal star polygons. Looking at these examples, one becomes aware that holes with high multiplicity seem to be morphologically more important than holes with low multiplicity.

4.2. *Snowflakes of the facet type*

Empirically, we have already found that snow crystals of the facet type have clear spots giving rise to analogous structural relations as the branching points of dendritic crystals. It is, therefore, natural to assume that in the facet-type snowflakes the orbit points are at potential minima, whereas the holes are at potential maxima. This would explain that impurities responsible for the internal dark lines avoid the hole positions. The clear spots now define the positions of the basic structural sites and the black lines have to be associated with lines connecting orbit points.

Starting with the sample BH 95.11 (Fig. 14*a*) already considered in Fig. 4, one is indeed able to assign to holes with sixfold multiplicity the light spots giving rise to three hexagonal star polygons: the largest one in vertex–vertex relation and the other two in vertex–mid-edge position with the set of scaled hexagons in which they are inscribed (Fig. 14*b*). At the same time, lines connecting orbit points allow reproduction, in a simplified but clear way, of the pattern of dark lines (Fig. 14*c*). From this, one sees that additional light spots,

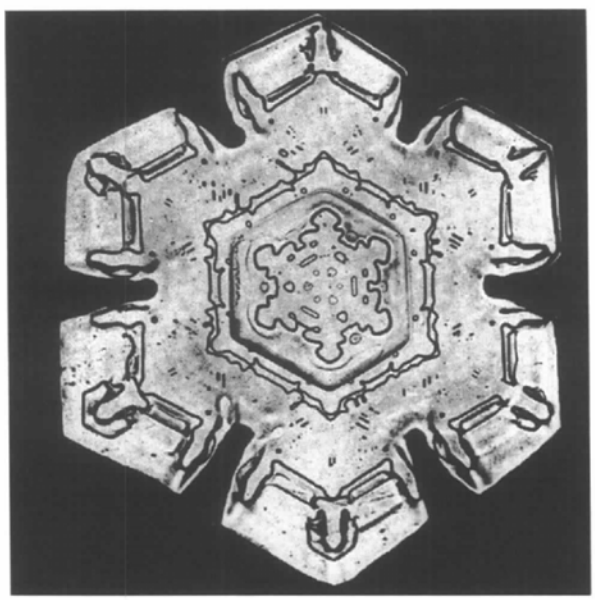

(*a*)

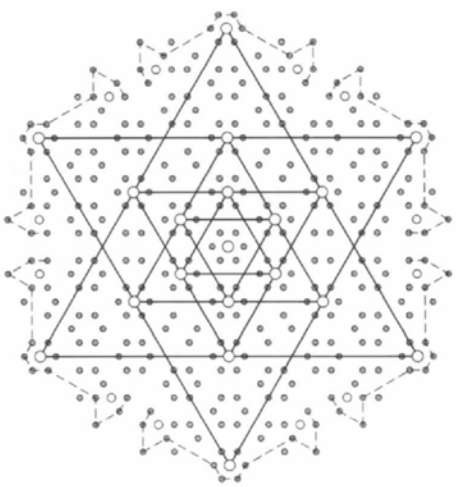

(*b*)

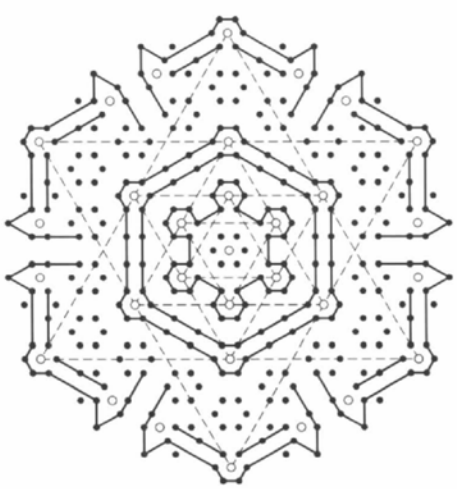

(*c*)

Fig. 14. (*a*) The snow crystal of facet type BH 95.11. (Courtesy of Dover.) (*b*) Interpretation of the light spots in terms of basic structural sites at hole positions. The corresponding skeleton gives rise to the set of scaled star hexagons already indicated in Fig. 4. A few more sites, clearly visible in the crystal, have also been included. (*c*) Interpretation of the internal dark lines, here obtained by connecting orbit points around the basic structural sites.

corresponding to holes with multiplicity 4, have to be included in the set of basic sites. Most significant is the agreement between the light and the dark patterns, and the fact that it is sufficient to fit the external boundaries for getting the internal structures at the right scale. In addition, this analysis reveals more structural relations than the few ones derived empirically in Fig. 4.

The sample SA 2 (shown in Fig. 15*a*), which was the starting point of this whole investigation, has essentially the same flower-like shape as the previous BH 95.11 one, but with a more elaborated internal structure. Even in this case, it is not difficult to identify in the snowflake the set of basic structural sites (Fig. 15*b*) in terms of holes of the orbit points and of corresponding light spots. What is even more important is that, by drawing lines between points of the given orbit (Fig. 15*c*), one gets many more structural relations than one would dare to ascribe to a single orbit of the multimetrical point group. In addition, the scaling relations empirically expressed for the dark-line patterns in Fig. 2 are interpreted at the same time as those among the clear spots indicated in Fig. 3. Again, more points appear to be at basic structural sites, the original set being that of the holes with the largest multiplicity, morphologically the more

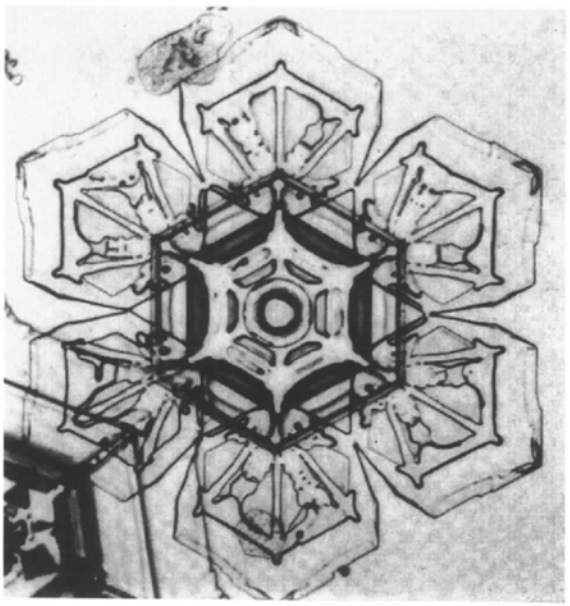

(*a*)

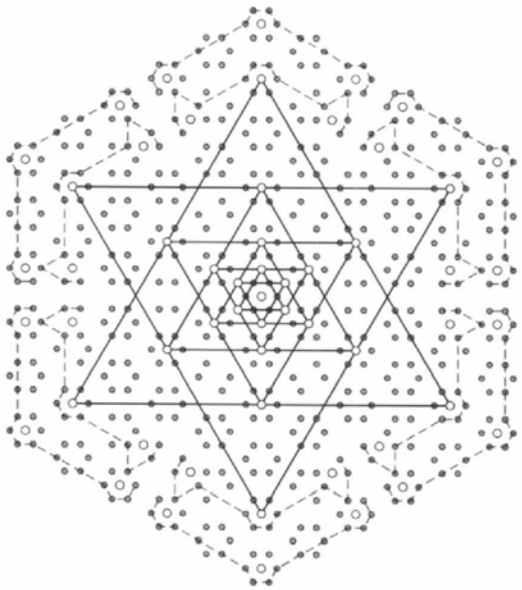

(*b*)

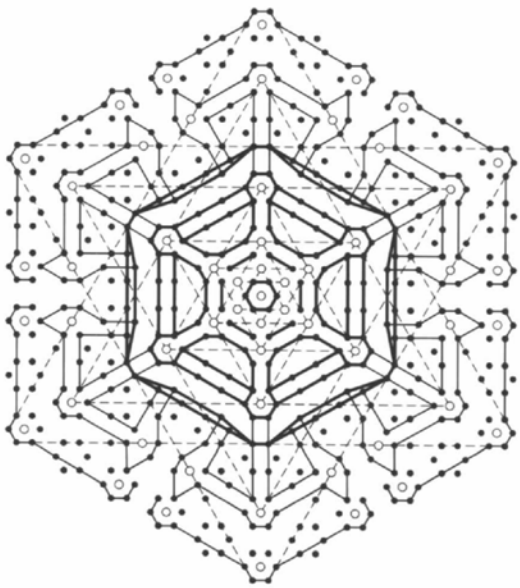

(*c*)

Fig. 15. (*a*) The same crystal SA 2 as shown in Figs. 2 and 3. (Courtesy of *Scientific American*.) (*b*) The set of light spots considered in Fig. 3 can be associated with holes of orbit points, in a way similar to that indicated in Fig. 14, with most of the spots at hexagonal holes and a few on rectangular holes of multiplicity 6 and 4, respectively. The hexagrammal structure indicated in Fig. 3 is here completed by additional relations among light spots, now visible, leading to an overall flower-like structure (indicated by dashed lines). (*c*) Identification of the rich pattern of internal dark lines.

important ones. One might object to a certain degree of arbitrariness in the identification of the orbit points to be connected for yielding the desired pattern of dark lines. This is, however, intrinsically required by the incredible variation in snowflakes, once their morphology is based on the geometry of the symmetry point group and on two singular points only: the origin $(0, 0)$ and the orbit starting point, say $(1, 0)$.

The third sample of the faced type considered (BH 58.11) is a variation of the previous crystal form and this is why it is an interesting case (Fig. 16*a*). The interpretation of its morphological features can be performed along the same principles. The result is shown in Figs.16(*b*), (*c*) and (*d*). The basic structural sites more easily identified are all holes with the maximal multiplicity six.

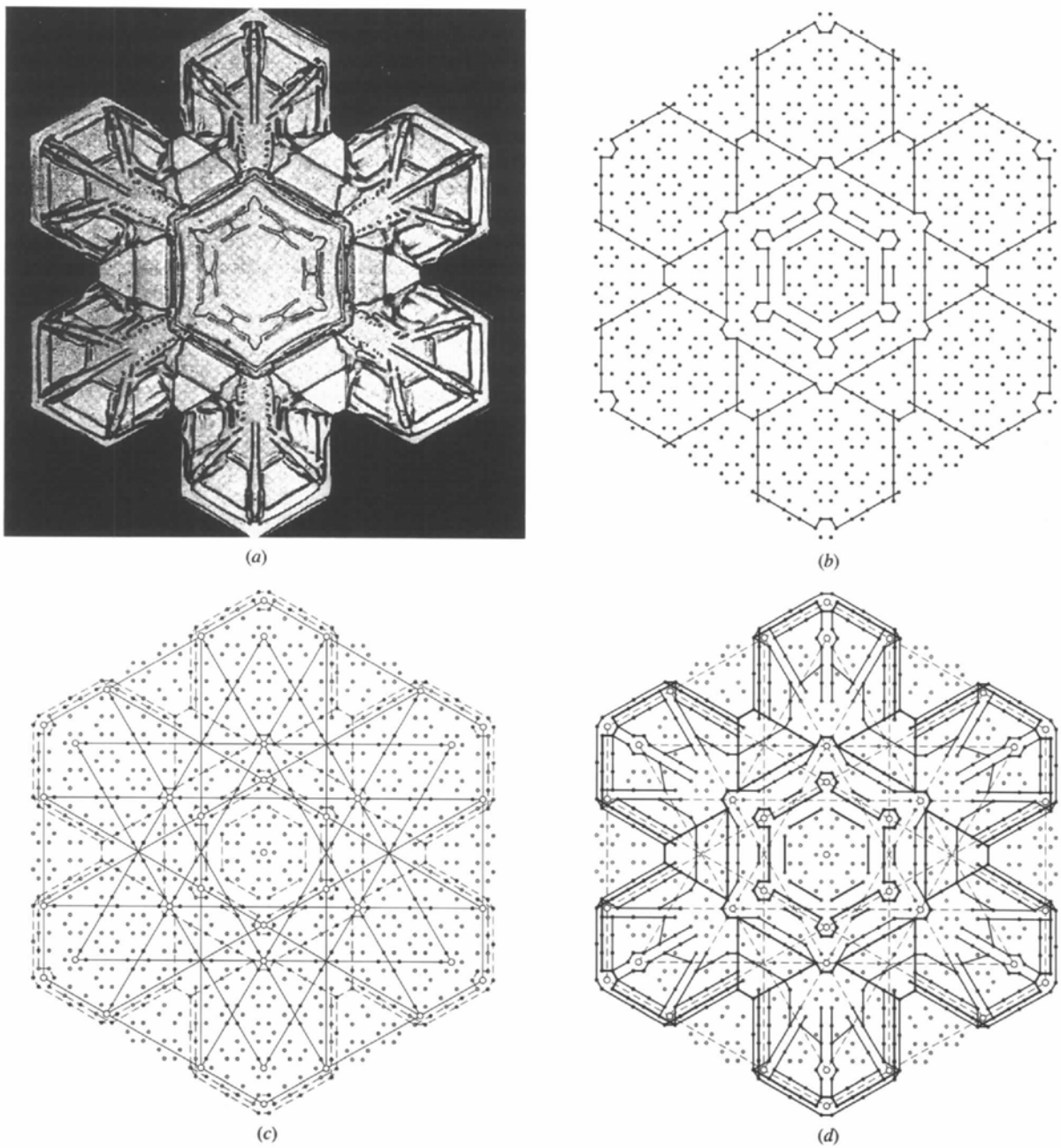

Fig. 16. (*a*) The flower-like snow crystal of the facet type BH 58.11. (Courtesy of Dover.) (*b*) Simplified pattern of the observed morphology in terms of orbit points. (*c*) Complex skeleton structure of the basic structural sites appearing in the crystal as light spots. (*d*) A more complete set of dark lines than the one given in (*b*), interpreting a type of pattern observed in many other snowflakes.

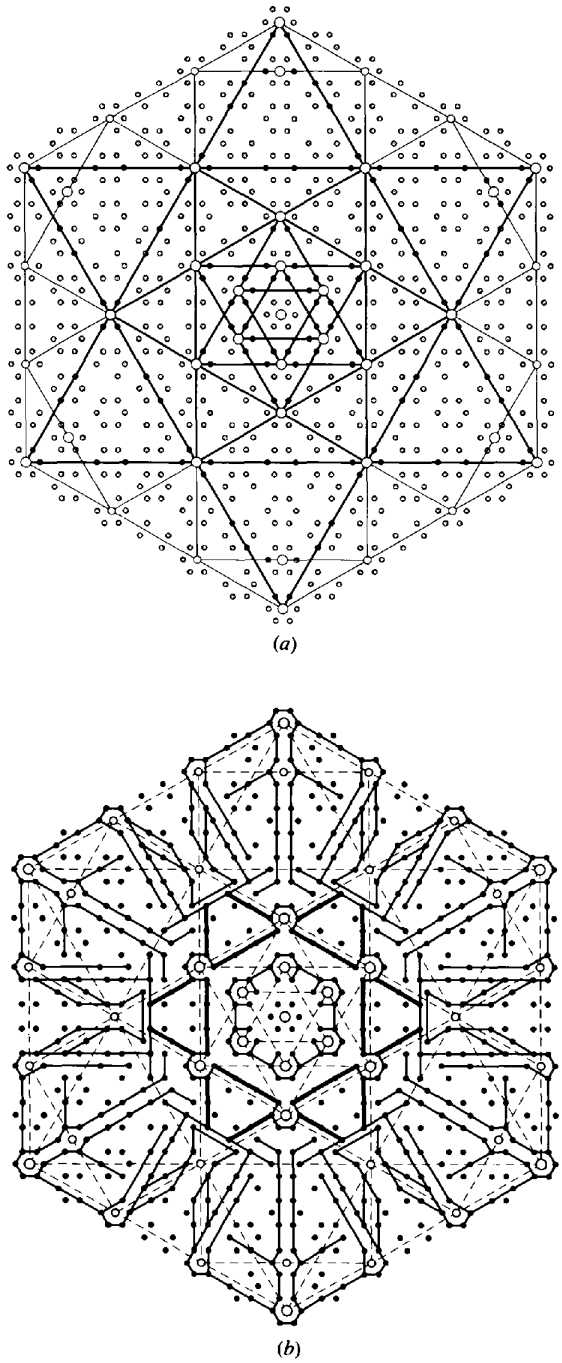

Fig. 17. Interpretation of the morphology of the crystal BH 141.11 already shown in Fig. 5. (*a*) Basic structural sites appearing as light spots in the crystal are indicated in their hexagrammal scaling relation. Most spots appear to be connected with the holes with the largest multiplicity. A few, less pronounced, are at holes with the lower multiplicity 4. Additional ones have multiplicity 5. (*b*) Interpretation of the pattern of dark lines in terms of lines connecting orbit points. The light spots are also indicated for demonstrating their perfect compatibility with the set of lines. Many details are here included, in a somewhat stylized realization, which nevertheless reproduces with the right size and at the right positions a great deal of the complex patterns observed in this snowflake.

The last and more complex example is the sample BH 141.11 already shown in Fig. 5 because of the explicit hexagonal star polygon appearing in it as a pattern of black lines. The corresponding interpretation is shown in Figs. 17(*a*) and (*b*). As one can see in this case as well, most of the morphological features can be interpreted on the basis of a single orbit. It is fair to remark that, for the set of parallel double lines appearing at the left and at the right of the hexagonal axes, the agreement between model and internal pattern is not always satisfactory.

4.3. *Morphological rules*

The morphological characterization of the seven snowflake samples discussed in the previous two subsections is summarized in Table 2.

It is certainly too early to formulate morphological laws on the basis of the data analyzed so far. An attempt is made here to formalize the observations by a number of rules. These rules have a geometrical character similar to that of Friedel's law (Friedel, 1907) and are not yet justified by physical processes like the ones considered by several authors for modeling dendritic growth (Ben-Jacob, 1993; Brener & Mel'nikov, 1991; Gonev & Kraus, 1994; Hurle, 1993; Kessler, Koplik & Levine, 1988; Langer, 1980; Nittmann & Stanley, 1987). In particular, the physical basis for the morphological relevance of non-Euclidean symmetry elements is totally missing.

Keeping this in mind, one can try to formulate some morphological rules.

Rule 1. A crystal form is based on two orbits of the multimetrical point group K of the crystal: the one-point orbit $O_K(0,0)$ of the origin and an infinite orbit $O_K(X)$ of a second (macroscopic) singular point X. This point can be assumed to be at an atomic position, point of the microscopic lattice Λ of symmetry translations.

The orbit $O_K(X)$ consists of points of a macroscopic lattice Λ_{cf} of the crystal form and is generated from a point $X(1,0) = Na_1 = (1,0)$, for N a large integer and a_1 a basis vector of the microscopic lattice Λ. This orbit is accordingly denoted by $O_K(1,0)$. The point $(1,0)$ fixes the natural unit of length of the crystal form.

Rule 2. Morphologically relevant are only the orbit points at a distance from the origin smaller than a given r_{max} related to the coherence length. This distance is typically of the order of 15 to 40 units.

Rule 3. A skeleton of the crystal form is defined in terms of basic structural sites, which are at hole positions of the orbit $O_K(1,0)$. These sites can be indexed by rational numbers by considering the hole positions with respect to Λ_{cf}. The basic structural sites have the Euclidean point-group symmetry K_0.

Table 2. *Crystal form characterization of snowflakes (Figs. 11 to 17)*

Sample	Form	r_{max}	Fig.	Basic structural sites (modulo $6m$) Multiplicity	Indices: $(m, n) \in HO_{6(4)m}(1, 0)$
SA 1	Dendritic	18	11	6	(0, 0) (4, 8) (8, 16) (10, 20) (8, 10) (12, 18)
BH 188.12	Dendritic	18	12	6	(2, 4) (4, 8) (8, 16) (10, 20) (12, 18)
				4	(3, 0) (6, 0) (12, 0)
BH 183.8	Dendritic	32	13	6	(2, 4) (4, 8) (6, 12) (8, 16) (10, 20) (12, 24) (16, 32) (18, 36) (20, 22)
				5	(14, 22) (20, 28)
				4	(1, 2) (6, 0) (12, 0) (18, 0) (20, 34)
BH 95.11	Facet	14	14	6	(0, 0) (2, 4) (4, 8) (8, 16)
				4	(11, 13)
SA 2	Facet	18	15	6	(0, 0) (2, 4) (4, 8) (8, 16) (10, 20) (14, 16)
				4	(1, 2) (11, 13)
BH 58.11	Facet	25	16	6	(0, 0) (4, 8) (6, 12) (12, 24) (14, 28) (18, 24)
BH 141.11	Facet	21	17	6	(0, 0) (2, 4) (4, 8) (10, 20) (12, 24)
				5	(4, 20)
				4	(12, 0)

Rule 4. Crystals of the dendritic type arise for $O_K(1, 0)$ at maxima of a not further specified potential, whereas an orbit of minima yields a crystal form of the facet type. In the dendritic case, the basic structural sites are at intersection points and at the end of dendritic branches. In the facet-type case, these sites appear as internal dots or pores. The internal line patterns can be modeled by connecting a selection of orbit points.

Rule 5. The morphological importance of a basic structural site increases with increasing hole multiplicity.

Rule 6. One can distinguish between homogeneous and inhomogeneous crystal growth forms. The homogeneous forms are classified by a set of symmetry-equivalent lattice planes. The inhomogeneous forms are characterized by a set of symmetry-equivalent lattice points.

Snow crystals of the dentritic and of the facet type are examples of inhomogeneous growth forms, whereas the columnar snow crystals (not considered in this paper) are expected to have homogeneous growth forms.

These rules have an indicative value allowing, in a number of cases, a symmetry interpretation to be given of the morphology of snow crystals that goes beyond the Euclidean point symmetry. No attempt has been made to estimate for how many of the more than 2000 snow crystals of the Bentley–Humphreys collection the present approach is valid, but certainly for many more samples than the few ones selected here.

5. Concluding remarks

The present approach explains, up to a certain degree, the geometry of snow crystals but not, however, the physics involved. The morphological interpretation of all the snow crystals considered is based on the fitting to the structure of two points only, the origin and one orbit or hole point of always the same set of admissible points. The deep meaning of the non-Euclidean symmetries for a Euclidean object, which is to express relevant Euclidean properties not due to Euclidean symmetries, gives the direction along which an interplay with physical laws can occur. A preliminary investigation has already demonstrated the possibility of interpreting some accidental degeneracy in energy band-structure calculations of crystals of the wurtzite structure type, on the basis of a multimetrical space group leaving the crystal structure invariant (Janner & Nusimovici, 1994).

The scaling properties observed in snow crystals are similar to those derived for Wyckoff positions in multimetrical space groups (Janner, 1995*a*). The positions for a given Wyckoff letter are not scaling invariant but there are families of Wyckoff positions in mutual scaling behavior. Here also, one orbit is not scaling invariant but gives rise to holes belonging to different orbits that are at mutually scaled positions.

APPENDIX *A*

The point group $K = 6(4)m$ expressed with respect to the hexagonal basis $a_1 = (1, 0)$ and $a_2 = (-1/2, 3^{1/2}/2)$ is a subgroup of $Gl(2, \mathbb{Z})$, the group of integral two-dimensional matrices with determinant ± 1. The corresponding proper subgroups are 6(4) and $Sl(2, \mathbb{Z}) = \Gamma$, respectively. The modular group Γ is generated by the two matrices [see Apostol (1976) and Schoeneberg (1974) for details]:

$$T = \begin{pmatrix} 1 & 1 \\ 0 & 1 \end{pmatrix} \quad \text{and} \quad S = \begin{pmatrix} 0 & \bar{1} \\ 1 & 0 \end{pmatrix}, \qquad (16)$$

whereas 6(4) is generated by

$$R(a) = \begin{pmatrix} 1 & \bar{1} \\ 1 & 0 \end{pmatrix} \quad \text{and} \quad L(a) = \begin{pmatrix} 3 & 1 \\ 2 & 1 \end{pmatrix}. \qquad (17)$$

The set of matrices $\begin{pmatrix} \alpha & \beta \\ \gamma & \delta \end{pmatrix}$ of Γ with $\beta = 0 \bmod 3$ forms a subgroup $\Gamma^0(3)$ of index 4 in Γ, with coset

decomposition

$$\Gamma = \Gamma^0(3)\left[\mathbb{1} + T + T^{-1} + S\right]. \qquad (18)$$

Proposition 1. The point group $6(4) = \langle R, L\rangle$, expressed with respect to the basis $c_1 = a_1$, $c_2 = a_2 - a_1$ is $\Gamma^0(3)$.

Proof: The group $\Gamma^0(3)$ is generated by $T' = S^{-1}TS$ and $V_2' = S^{-1}V_2S$ with

$$T' = \begin{pmatrix} 1 & 0 \\ \bar{1} & 1 \end{pmatrix} \quad \text{and} \quad V_2' = \begin{pmatrix} 1 & 1 \\ \bar{3} & \bar{2} \end{pmatrix}. \qquad (19)$$

[See (Apostol, 1976, p. 79) using $\Gamma_0(3) = S^{-1}\Gamma^0(3)S$.] One then verifies the relations:

$$\begin{aligned} R(c) &= TR(a)T^{-1} = -V_2', \\ L(c) &= TL(a)T^{-1} = -V_2'(T')^{-1}. \end{aligned} \qquad (20)$$

Corollary. The group 6(4) is isomorphic to a subgroup of index 4 in Γ and the group $K = 6(4)m$ is isomorphic to a subgroup of index 4 in $Gl(2, \mathbb{Z})$. When referred to the hexagonal basis, $K(a)$ has the coset decomposition:

$$Gl(2, \mathbb{Z}) = K(a)\left[\mathbb{1} + T + T^{-1} + T^{-1}S\right]. \qquad (21)$$

The fundamental region of $6(4)/\{\pm\mathbb{1}\}$, considered as the group of fractional linear transformations acting on the extended upper half complex plane, is the union of the fundamental region I of the modular group and the corresponding images by T, T^{-1} and $T^{-1}S$ (Fig. 18).

Proposition 2. The hexagonal lattice points (m, n) of the two orbits $O_{6(4)}(\bar{1}, 1)$ and $O_{6(4)}(1, 0)$ satisfy the condition g.c.d.$(m, n) = 1$. The congruence $2m - n = 0 \bmod 3$ characterizes the points allowed for $O_{6(4)}(\bar{1}, 1)$ and forbidden for $O_{6(4)}(1, 0)$.

Proof: A point (m, n) of the hexagonal lattice (referred to the basis a), when expressed in the basis c, yields: $(m, n) = (m+n, n)_c$. The image of $(p, q)_c$ by an element of $\Gamma^0(3)$ is:

$$\begin{pmatrix} \alpha & 3\beta \\ \gamma & \delta \end{pmatrix}\begin{pmatrix} p \\ q \end{pmatrix}_c = \begin{pmatrix} \alpha p + 3\beta q \\ \gamma p + \delta q \end{pmatrix}_c = \begin{pmatrix} m+n \\ n \end{pmatrix}_c \qquad (22)$$

so that $m = (\alpha - \gamma)p + (3\beta - \delta)q$ and $n = \gamma p + \delta q$. Accordingly, $2m - n = 2\alpha p \bmod 3$. The orbit of the point $(1, 0)$ by Γ splits into the orbit of $(0, 1)_c = (\bar{1}, 1)$ and of $(1, 0)_c = (1, 0)$, respectively. In the first case, $p = 0$ so that the congruence $2m - n = 0 \bmod 3$ allows the points for the first orbit and forbids those of the second orbit.

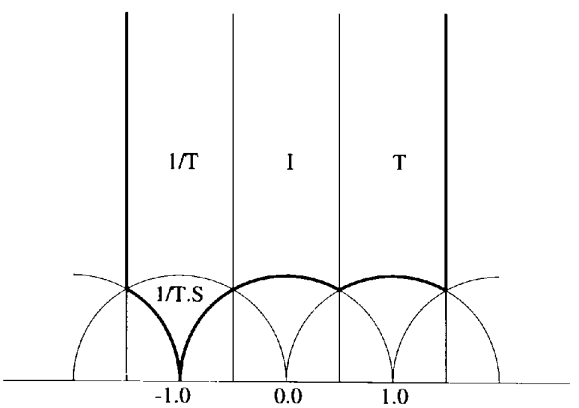

Fig. 18. Fundamental region (indicated by heavy lines) of the multimetrical hexagonal point group 6(4) acting as a group of fractional linear transformations on the upper half complex plane. The fundamental region I of the modular group is indicated together with the images of I obtained from the coset representatives T, T^{-1} and $T^{-1}S$.

Thanks are expressed to J. M. Thijssen for his flexible and practical program *XPS* used for the drawings; to C. Beeli for information on snow crystals observed by scanning electron microscopy (Wergin, Rango & Erbe, 1995); to J. Mennicke for a kind invitation to Bielefeld, where I learned properties of indefinite integral quadratic forms, and to H. Helling of the same Mathematical Institute for indicating the relation between the groups $\Gamma^0(3)$ and 6(4) of Proposition 1. The encouragements of Annalisa Fasolino and the stimulating discussions with A. Thiers are gratefully acknowledged.

References

Apostol, T. M. (1976). *Modular Functions and Dirichlet Series in Number Theory*. Berlin: Springer-Verlag.
Ben-Jacob, E. (1993). *Contemp. Phys.* **34**, 247–273.
Bentley, W. A. & Humphreys, W. J. (1931). *Snow Crystals*. New York: McGraw-Hill. New York: Dover (1962).
Bernal, J. D. & Fowler, R. H. (1933). *J. Chem. Phys.* **1**, 515–548.
Brener, E. A. & Mel'nikov, V. I. (1991). *Adv. Phys.* **40**, 53–97.
Conway, J. H. & Sloane, N. J. A. (1988). *Sphere Packings, Lattices and Groups*. Berlin: Springer-Verlag.
Frank, F. C. (1982). *Contemp. Phys.* **23**, 3–22.
Friedel, G. (1907). *Bull. Soc. Fr. Minéral.* **30**, 326.
Gonev, N. & Kraus, I. (1994). *IUCr Newsletter*, **2**(3), 12.
Hurle, D. T. J. (1993). *Handbook of Crystal Growth*. Amsterdam: Elsevier Science B.V.
Janner, A. (1991*a*). *Phys. Rev. Lett.* **67**, 2159–2162.
Janner, A. (1991*b*). *Phys. Rev. B*, **43**, 13206–13214.
Janner, A. (1992). *Acta Cryst.* A**48**, 884–901.
Janner, A. (1995*a*). *Acta Cryst.* B**51**, 386–401.
Janner, A. (1995*b*). *Beyond Quasicrystals*, edited by F. Axel & D. Gratias, pp. 33–54. Les Ulis: Les Editions de Physique; Berlin: Springer.
Janner, A. & Nusimovici, M. A. (1994). *Theories of Matter: a Festschrift for Professor Joseph L. Birman*, edited by A. Solomon, M. Balkanski & H.-R. Trebin, pp. 98–118. Singapore: World Scientific.

Kepler, J. (1611). *Strena Seu De Nive Sexangula*. Frankfurt am Main: Godfrey Tampach. Engl. transl: *The Six-Cornered Snowflake*. Oxford: Clarendon Press (1966).
Kessler, D. A., Koplik, J. & Levine, H. (1988). *Adv. Phys.* **37**, 255–339.
Langer, J. S. (1980). *Rev. Mod. Phys.* **52**, 1–28.
Mason, B. J. (1961). *Scientific American*, January, pp. 120–131.
Nakaya, U. (1954). *Snow Crystals*. Cambridge: Harvard University Press.
Nittmann, J. & Stanley, H. E. (1987). *J. Phys. A: Math. Gen.* **20**, L1185–L1191.
Pauling, L. (1935). *J. Am. Chem. Soc.* **57**, 2680–2684.
Peterson, S. W. & Levy, H. A. (1957). *Acta Cryst.* **10**, 70–76.
Schoeneberg, B. (1974). *Elliptic Modular Functions*. Berlin: Springer-Verlag.
Steurer, W. (1991). *J. Phys. Condens. Matter*, **3**, 3397–3410.
Wergin, W. P., Rango, A. & Erbe, E. F. (1995). *Scanning*, **17**, 41–49.